

WFUMB GUIDELINES AND RECOMMENDATIONS FOR CLINICAL USE OF ULTRASOUND ELASTOGRAPHY: PART 1: BASIC PRINCIPLES AND TERMINOLOGY

TSUYOSHI SHIINA, PhD,¹ KATHRYN R. NIGHTINGALE, PhD,² MARK L. PALMERI, MD, PhD,²
TIMOTHY J. HALL, PhD,³ JEFFREY C. BAMBER, PhD,⁴ RICHARD G. BARR, MD, PhD,⁵
LAURENT CASTERA, MD,⁶ BYUNG IHN CHOI, MD,⁷ YI-HONG CHOU, MD,⁸ DAVID COSGROVE, MD,⁹
CHRISTOPH F. DIETRICH, MD, PhD,¹⁰ HONG DING, MD,¹¹ DOMINIQUE AMY, MD,¹²
ANDRE FARROKH, MD,¹³ GIOVANNA FERRAIOLI, MD,¹⁴ CARLO FILICE, MD,¹⁴
MIREEN FRIEDRICH-RUST, MD,¹⁵ KAZUTAKA NAKASHIMA, MD, PhD,¹⁶ FRITZ SCHAFFER, MD,¹⁷
IOAN SPOREA, MD, PhD,¹⁸ SHINICHI SUZUKI, MD,¹⁹ STEPHANIE WILSON, MD,²⁰
and MASATOSHI KUDO, MD, PhD²¹

¹Department of Human Health Sciences, Graduate School of Medicine, Kyoto University, Kyoto, Japan; ²Department of Biomedical Engineering, Duke University, Durham, NC, USA; ³Department of Medical Physics, University of Wisconsin-Madison, Madison, WI, USA; ⁴Joint Department of Physics, Institute of Cancer Research and Royal Marsden NHS Foundation Trust, Sutton, London, UK; ⁵Department of Radiology, Northeastern Ohio Medical University, Rootstown, Ohio and Radiology Consultants Inc., Youngstown, Ohio, USA; ⁶Service d'Hépatologie, Hôpital Beaujon, Clichy, Assistance Publique-Hôpitaux de Paris, INSERM U 773 CRB3, Université Denis Diderot Paris-VII, France; ⁷Department of Radiology, Seoul National University Hospital, Seoul, Korea; ⁸Department of Radiology, Veterans General Hospital and National Yang-Ming University, School of Medicine, Taipei; ⁹Imaging Departments, Imperial and Kings Colleges, London, United Kingdom; ¹⁰Medizinische Klinik 2, Caritas-Krankenhaus Bad Mergentheim, Germany; ¹¹Department of Ultrasound, Zhongshan Hospital, Fudan University, China; ¹²Breast Center, 21 Ave V. Hugo 13100 Aix-en-Provence, France; ¹³Department of Gynecology and Obstetrics, University Hospital RWTH Aachen, Germany; ¹⁴Ultrasound Unit - Infectious Diseases Department, Fondazione IRCCS Policlinico San Matteo - University of Pavia, Italy; ¹⁵Department of Internal Medicine 1, J. W. Goethe University Hospital, Theodor-Stern-Kai 7, 60590 Frankfurt am Main, Germany; ¹⁶Department of General Surgery, Kawasaki Medical School, Okayama, Japan; ¹⁷Department of Breast Imaging and Interventions, University Hospital Schleswig-Holstein Campus Kiel, Germany; ¹⁸Department of Gastroenterology and Hepatology, University of Medicine and Pharmacy Timișoara, Romania; ¹⁹Department of Thyroid and Endocrinology, Fukushima Medical University, School of Medicine, Fukushima, Japan; ²⁰Department of Diagnostic Imaging, Foothills Medical Centre, University of Calgary, Calgary, AB, Canada; and ²¹Department of Gastroenterology and Hepatology, Kinki University School of Medicine, Osaka-Sayama, Osaka, Japan

Abstract—Conventional diagnostic ultrasound images of the anatomy (as opposed to blood flow) reveal differences in the acoustic properties of soft tissues (mainly echogenicity but also, to some extent, attenuation), whereas ultrasound-based elasticity images are able to reveal the differences in the elastic properties of soft tissues (e.g., elasticity and viscosity). The benefit of elasticity imaging lies in the fact that many soft tissues can share similar ultrasonic echogenicities but may have different mechanical properties that can be used to clearly visualize normal anatomy and delineate pathologic lesions. Typically, all elasticity measurement and imaging methods introduce a mechanical excitation and monitor the resulting tissue response. Some of the most widely available commercial elasticity imaging methods are ‘quasi-static’ and use external tissue compression to generate images of the resulting tissue strain (or deformation). In addition, many manufacturers now provide shear wave imaging and measurement methods, which deliver stiffness images based upon the shear wave propagation speed. The goal of this review is to describe the fundamental physics and the associated terminology underlying these technologies. We have included a questions and answers section, an extensive appendix, and a glossary of terms in this manuscript. We have also endeavored to ensure that the terminology and descriptions, although not identical, are broadly compatible across the WFUMB and EFSUMB sets of guidelines on elastography (Bamber et al. 2013; Cosgrove et al. 2013). (E-mail: shiina.tsuyoshi.6w@kyoto-u.ac.jp) © 2015 Published by Elsevier Inc. on behalf of World Federation for Ultrasound in Medicine & Biology.

Keywords: ultrasonography, elasticity, stiffness, elastogram, elastography, strain, shear wave, acoustic radiation force, transient elastography.

INTRODUCTION

It is known that changes in tissue stiffness are involved in various diseases such as cancerous masses, fibrosis associated with liver cirrhosis, and atheroma and calcification associated with arteriosclerosis. While a variety of techniques such as CT, MRI, and PET are being put to practical use for diagnostic imaging of morphology and function, a technique for objectively assessing tissue stiffness was only recently made widely available with the commercial introduction of ultrasound elastography. Some examples of the clinical usefulness of tissue stiffness measurement are:

- 1) Use in early detection and differential diagnosis of diseases because it may reflect qualitative changes even when morphological changes are not apparent.
- 2) Improvement in accuracy for diagnosing diseases involving fibrosis, such as cancer, chronic hepatitis and atherosclerosis, by evaluating the extent of lesions and the degree of progression.
- 3) Assessment of response to treatments, such as radio-frequency ablation and chemotherapy.

In elastically uniform materials, stiffness can easily be expressed using the elastic modulus as described in Section 2.1; however, in the case of biological tissues, there are a variety of factors that determine stiffness including the tissue's fatty and fibrous constituents. For example, it is known that atherosclerotic plaques become stiffer with disease progression as their composition changes from lipid to fibrosis and calcified tissue. At the macroscopic level, it is known that the tissue in the margins around a malignant breast tumor is resistant to deformation and feels hard during palpation; therefore, tissue elasticity will differ depending on the microscopic or macroscopic observation. Moreover, the elasticity of biological tissue, which is anisotropic, viscous and nonlinear, will differ depending on the direction, extent and rate of deformation. Nevertheless, even when the elastic modulus is determined using the assumption that it is independent of these variables, it shows a high correlation with disease. As shown in Table 1, the results of mechanical measurement of resected breast cancer tissue

(DCIS: ductal carcinoma in situ, IDC: invasive ductal carcinoma) showed that its elastic modulus (Young's modulus) was significantly higher than that of normal glandular tissue (Krouskop *et al.* 1998; Wellman *et al.* 1999; Samani *et al.* 2007).

PRINCIPLES OF ELASTOGRAPHY

Measured physical quantity and excitation methods

Differences in the elasticity of soft tissues are expressed by elastic moduli such as Young's modulus (E) and shear modulus (G), which indicate how difficult it is to deform tissues via compression and shear, respectively. In the commercially available elasticity imaging systems, these moduli are typically calculated using one of the following methods with respect to the directly measured quantity of tissue deformation (see the relational equations in Appendix):

- 1) Calculate E using the following equation (Hooke's law, Eq. (A1) in Appendix) after externally applying stress σ and measuring strain ϵ ,

$$E = \sigma / \epsilon \quad (1)$$

- 2) Calculate E or G using Eq. (2) (derived from Appendix Eqs. (A7) and (A9)) after propagating shear waves (transverse waves) and measuring the propagation speed c_s .

$$E = 2(1+\nu)G = 3G = 3\rho c_s^2 \quad (2)$$

Here, we assume that Poisson's ratio (ν) of soft tissue is near 0.5 for an incompressible medium, which is a good approximation (Eq. (A7)), and ρ is the tissue density. Thus, Young's modulus will be equal to about three times the shear modulus for most assumed incompressible and isotropic tissues.


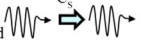
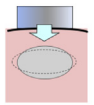
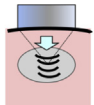
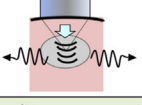
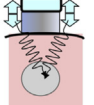
Although work on ultrasonic assessment of tissue elasticity dates back to the 1970s (Bamber 1999), research on both of the above methods started at the same time in the early 1990s (Ophir *et al.* 1991; Parker *et al.* 1990, 2011). The former was called the quasi-static method and the latter the dynamic method according to how the external mechanical excitation was applied, but subsequently these have been referred to as **strain imaging** and **shear wave imaging**, respectively, based on the measured quantity.

Both strain and shear wave imaging require mechanical excitation that can be divided into (A) Manual compression (by hand or using cardiovascular pulsation or respiratory motion), (B) Acoustic Radiation Force Impulse, and (C) External mechanical vibration. Elastography is generally classified by the differences in the measured physical quantity, the excitation method, and the method of displaying the measured quantity

Table 1. Young's modulus of breast tissue samples (Samani *et al.* 2007)

Breast tissue type	Young's modulus: Mean \pm SD (kPa)
Normal fat	3.25 \pm 0.91
Normal fibroglandular tissue	3.24 \pm 0.61
Fibroadenoma	6.41 \pm 2.86
DCIS	16.38 \pm 1.55
Low-grade IDC	10.40 \pm 2.60
High-grade IDC	42.52 \pm 12.47

Table 2a. Elastography methods. Each column shows methods and measured physical quantities for elastography. Each row shows methods for inducing displacement. Each cell shows a type of elastography.

Measured physical quantity Methods	Strain or Displacement 		Shear wave speed 	
	Strain imaging		Shear wave imaging	
Excitation methods	Strain elastography		N/A	
(A) Manual compression -Palpation, -Cardiovascular pulsation -Respiration	ElaXio™ Real-time tissue elastography™ Elastography ElastoScan™ eSieTouch™Elasticity Imaging 	Esaote Hitachi Aloka GE, Philips,Toshiba Ultronix, Mindray Samsung Siemens		
	(B) Acoustic radiation force impulse excitation	*ARFI Imaging		**Point shear wave speed measurement (Average shear wave speed in a region of interest)
Virtual Touch™Imaging(VTI/ARFI) 		Siemens	Virtual Touch™Quantification (VTQ/ARFI) ElastPQ™ 	Siemens Philips
		Shear wave speed imaging		
		ShearWave™Elastography: (SWE™) Virtual Touch™ Image Quantification (VTIQ/ARFI)	SuperSonic-Imagine Siemens	
(C) Controlled external vibration			***Transient elastography (Point shear wave speed measurement)	
			FibroScan™ 	Echosens

*The term ‘ARFI’ is often employed to refer to methods that use ARFI excitation independent of the physical quantity that is being measured (i.e., both for methods measuring strain/displacement and methods measuring shear wave speed), whereas the term ‘ARFI Imaging’ specifically refers to the use of an ARFI excitation and the subsequent measurement/display of tissue displacement or related physical quantity within the ARFI push region. Methods that employ an ARFI excitation and report shear wave speed have also been referred to as quantitative ARFI methods.

**The term point shear wave measurement has been introduced for the method where a local average of shear wave speed is determined using ARFI excitation with subsequent monitoring of the shear wave propagation outside of the push location throughout a specified region of interest that is presumed to be homogeneous (typically ~1 cm²).

***Transient elastography (TE) also performs point shear wave speed measurement (a term that has been introduced subsequent to the development of TE), but its name refers to the excitation method (i.e., the dynamic nature of the vibration in contrast to the quasi-static excitation used in strain imaging), rather than the physical quantity that is being measured.

(Table 2a). Methods that have been integrated into clinical practice can be categorized into the following groups:

- 1) Strain elastography
Strain induced by quasi-static methods such as manual compression or cardiovascular/respiratory pulsation is estimated, and the distributions of strain or normalized strain values within the ROI are displayed.
- 2) Transient elastography

- 3) Acoustic Radiation Force Impulse (ARFI) Imaging
Focused acoustic radiation force ‘pushing’ pulses are used to deform the tissue. The resulting tissue

A controlled vibrating external ‘punch’ is used to generate shear waves, and the average shear wave speed within an ROI is measured and converted to Young’s modulus using Eqn. (2). At present, commercialized technology is specialized for measuring the stiffness of liver tissue and not for imaging.

displacement is measured within the focal region of each push within a specified ROI, and the distribution of displacement or its normalized values within the ROI is displayed. This imaging method provides similar information as the strain images of Group 1 because both strain and displacement are inversely related to tissue stiffness, and neither method provides a quantitative estimate of the tissue elastic moduli because they are both affected by tissue geometry.

- 4) Shear wave speed measurement and imaging using acoustic radiation force impulse excitation
 Focused acoustic radiation force pushing pulses of short duration (i.e., temporal impulse, < 1 ms) are used to generate shear waves within an organ of interest, and the speed of the shear waves propagating away from the pushing location is measured. The information can be reported as either an average value within an ROI (a point measurement) or as an image, and the values are reported as either shear wave speed or converted to elastic modulus using Eq. (2).

Outputs obtained from each of these elastography techniques correspond to a measured physical quantity, as shown in Table 2b. For strain, geometric measures include the size or shape of the low strain area, strain ratio of the lesion to reference and E/B size ratio (ratio of the size of a lesion in the strain image to its size in the B-mode image). For shear wave speed-based methods, the physical quantity is speed itself, and/or Young’s modulus converted from shear wave speed on assumptions of constant density, homogeneity, isotropy, and incompressibility using Eq. (2). The characteristics of each technology are described below.

STRAIN AND DISPLACEMENT

Strain elastography

The first style of elastography put to practical use is a method for measuring the tissue deformation generated by applying pressure with a probe on the body surface. It is classified as **strain elastography** in Table 2a.

As shown in Figure 1, when a very slight pressure is applied to tissue with a probe in the beam direction, displacement $\delta(z)$ at each site z is calculated by comparing the echo signal before and after compression. Next, strain (ϵ), the deformation ratio between two adjacent points with interval, L , is obtained as shown in Eq. (3):

$$\epsilon = \frac{d\delta}{dz} \rightarrow \frac{\delta_2 - \delta_1}{L} \tag{3}$$

As shown in Eq. (1), Young’s modulus E can be obtained if stress σ and strain ϵ are known; however, because it is difficult to actually calculate the stress distribution *in vivo*, it is assumed to be uniform. As a result, stiff segments with a large elastic modulus E will have a small strain ϵ ; therefore, strain represents relative stiffness.

Strain imaging was first developed in the 1970s and named **elastography** by Dr. Jonathan Ophir (Ophir *et al.* 1991). Through various investigations of approaches for measurement of strain and its imaging (Bamber *et al.*, 1996; Shiina *et al.*, 1996; Varghese *et al.*, 1997; Bamber *et al.*, 2002; Hall *et al.*, 2003), the method of strain elastography has been commercialized, with the pressure applied manually, similar to palpation, or by cardiovascular pulsation and is currently being used in various fields of clinical medicine, including breast cancer diagnosis (Hall *et al.* 2003; Itoh A, *et al.* 2006).

Table 2b. Elastography output. Each column shows methods for elastography. Each row shows methods for inducing displacement. Each cell shows one or more outputs. The table is designed to be read in conjunction with Table 2a.

Methods Excitation method	Strain imaging	Shear wave imaging
(A) Manual compression Palpation, Cardiovascular pulsation Respiratory	Strain elastography Strain or normalized strain Geometric measures Strain ratio E/B size ratio	
(B) Acoustic radiation force impulse excitation	ARFI Imaging Displacement or normalized displacement Geometric measures Displacement ratio E/B size ratio	Point shear wave speed measurement Shear wave speed (m/s) Young’s modulus (kPa) Shear wave speed imaging Shear wave speed (m/s) Young’s modulus (kPa)
(C) Mechanical external vibration		Transient Elastography Young’s modulus (kPa)

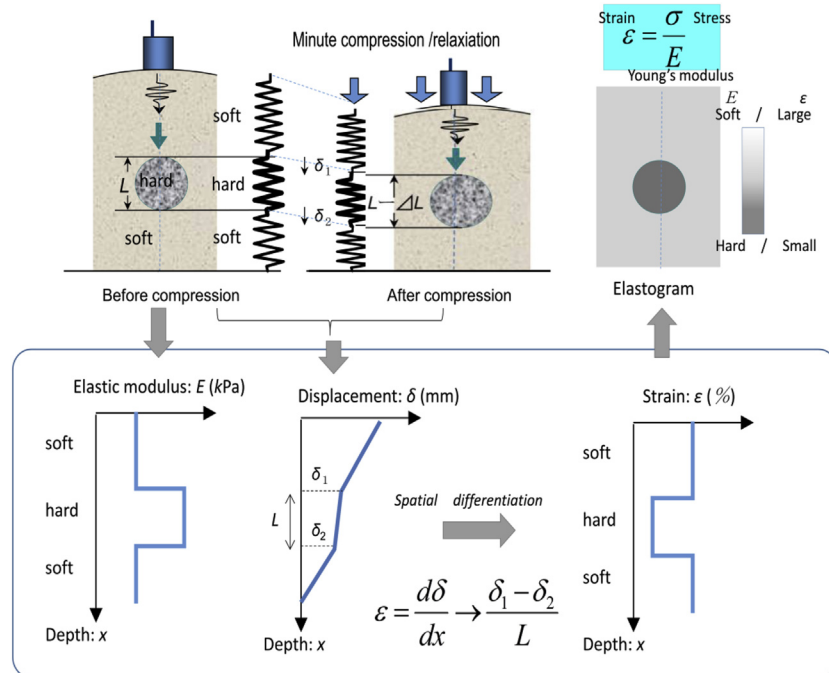


Figure 1. Principle of strain elastography. When very slight pressure (approximately 1%; e.g., for a typical breast depth of 3 cm, a compression of 1% would be 0.3 mm) is applied to tissue with a probe in the beam direction, the majority of the displacement will be in the direction of the propagation of the ultrasound pulse, and the tissue deformation can be approximated using a 1D spring model. Displacement $\delta(z)$ at each site z in the beam direction of the tissue is then calculated. This is obtained by calculating the correlation between the echo signal before and after compression. Next, strain ϵ is obtained by spatial differentiation (gradient) of displacement, that is, a ratio of the difference in displacement between two points to their distance pre-compression, L .

With respect to manual compression of the body surface, it is possible to apply pressure up to the normal diagnostic depth of superficial organs such as the breast and thyroid gland; however, stress is not easily transmitted to deep organs such as the liver, making it difficult to elicit strain. Therefore, strain induced by either cardiovascular pulsation or respiration is used for evaluation of liver fibrosis with strain imaging (Morikawa et al. 2011).

Commercial system of strain elastography

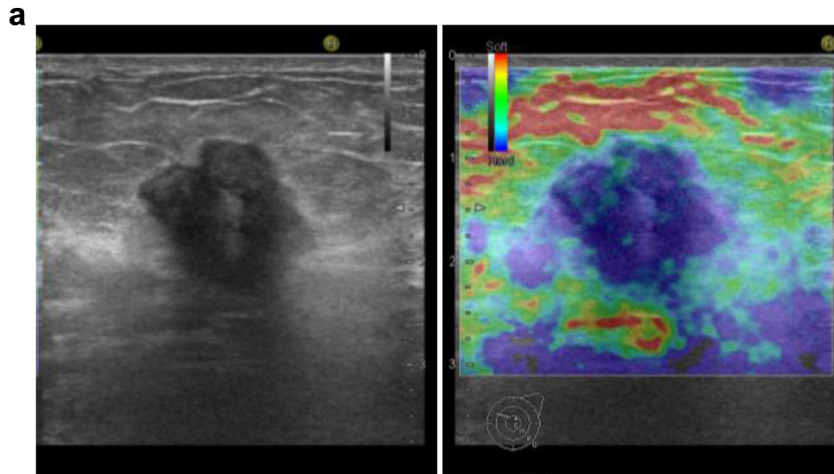
The first commercial sale of ultrasound elastography was for strain elastography in 2003, employing manual compression with a probe. The efficacy of this system was demonstrated in the diagnosis of breast cancers together with the "Tsukuba (elasticity) score" (Shiina et al. 2002; Itoh et al. 2006). Strain imaging has the advantages of being easy to use and provides elasticity images with a high spatial resolution in a manner similar to palpation (i.e., tissue deformation). Currently, many manufacturers produce ultrasonographic equipment with a strain elastography function.

Display methods for strain images. Strain is a relative indicator of stiffness, which changes depending on the degree of compression. For example, the **elastogram**

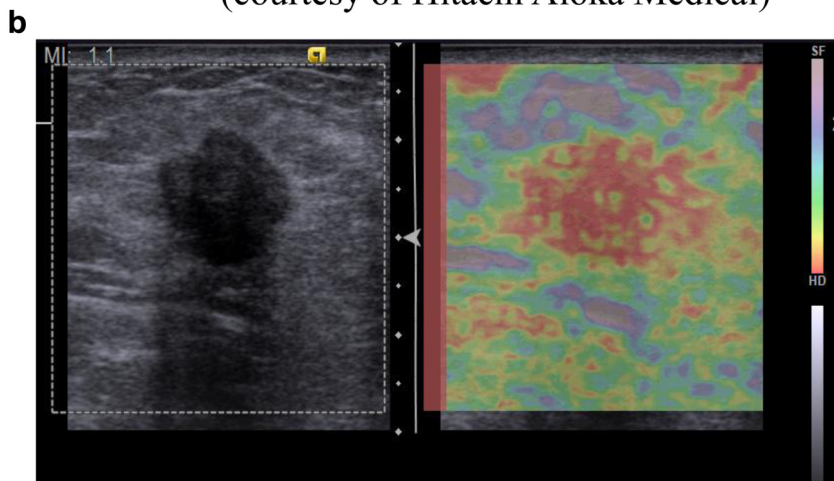
(strain image) shown in Figure 2(a) displays the normalized strain as the mean within the ROI to obtain a stable image without being subjected to fluctuations in the intensity of compression.

For clinical use, the display method of the elastogram is an important factor because it is useful for diagnosis to easily relate the location in the elastogram to the B-mode morphology. It is common to superimpose a translucent colored elastogram on the B-mode image. Dr. Ueno (Itoh et al. 2006) proposed a color scale that was applied to the first widely available commercial system (Figure 2(a)). At present, different color or gray scale displays are used for different ultrasonographic equipment (Figure 2(b)). In most equipment, users can select the color scale as desired.

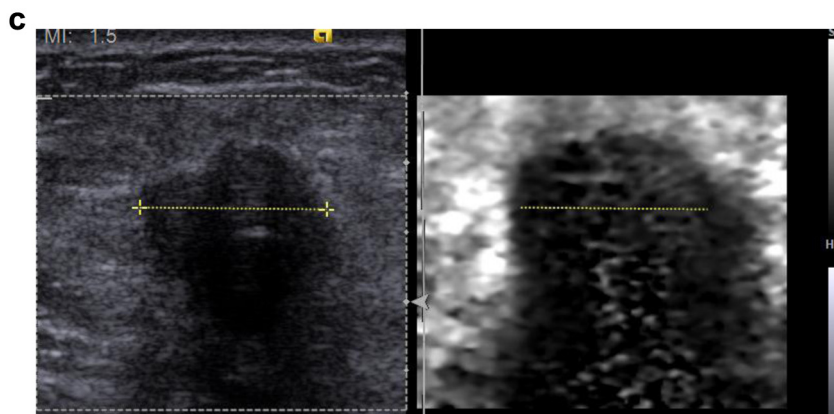
Trial of quantitative evaluation based on strain elastography. As mentioned above, strain imaging is essentially qualitative because its quantification requires knowledge about the stress distribution within the body, so it is difficult to perform quantitative comparisons between cases. There are some approaches to solving inverse problems which estimate quantitatively elastic modulus from strain or displacement under certain assumptions (Barbone et al., 2004; Fehrenbach et al., 2007). However clinical application of those methods



B-mode (breast cancer) Elastogram
Color elastogram superimposed on B-mode image
(courtesy of Hitachi Aloka Medical)



Elastogram in a different color scale
(courtesy of Siemens)



Elastogram in gray scale. (courtesy of Siemens)

Figure 2. Display methods of strain image. (a) Elastogram displays the normalized strain as the mean within the ROI to obtain stable images without being subjected to fluctuations in the intensity of compression. The translucent colored elastogram within the ROI is superimposed on the corresponding B-mode image; the average strain in the ROI is indicated in

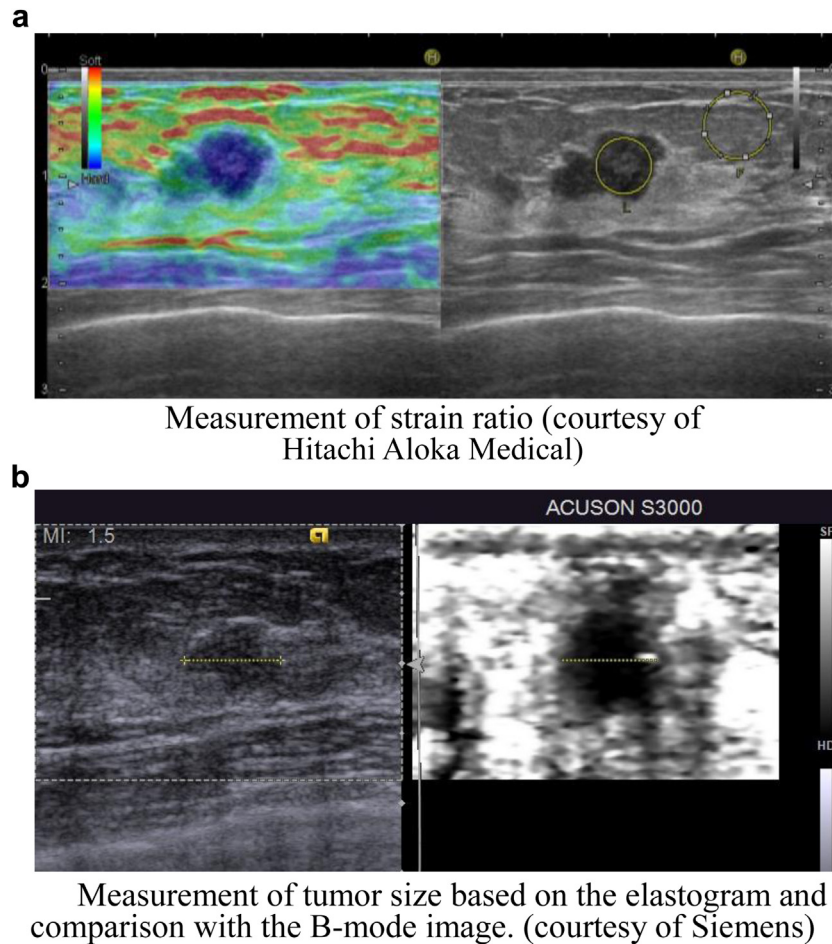


Figure 3. Quantitative diagnosis based on strain elastography. (a) The fat lesion ratio (FLR) is the strain ratio between the fat and the lesion based on the fact that the change in elasticity of fat caused by disease is minimal. (b) The size of the tumor in an elastogram is often measured and compared with the size of the low-echo area in B-mode (Matsumura et al. 2009).

are still being investigated. Therefore, pseudo-quantitative methods such as the **strain ratio**, (Figure 3(a)) (Ueno et al. 2007; Farrokh et al. 2011) and the ratio of the size of the tumor in an elastogram to the size of the low-echo area in B-mode (Garra et al. 1997) (Figure 3(b)) have been used.

Elasticity score. Strain images depict the relative difference in elasticity between a lesion, such as a mass and the surrounding tissue, making it suitable for detecting patterns in images. In practice, the elasticity score (Tsukuba score) is widely used for breast cancer diagnosis (Itoh et al. 2006) (Figure 4).

ARFI Imaging

A method called **acoustic radiation force impulse (ARFI) imaging** that images the tissue deformation

induced using focused ultrasound beams has been devised (Nightingale et al., 2001, Nightingale et al., 2002) and is commercially available. Imaging pulses before and after application of focused acoustic radiation force ‘push’ pulses are used to monitor the tissue displacement (as a measure of deformation) within the region of the ‘push’ (see Section 4.2 for a description of acoustic radiation force). The same transducer is used to generate the push pulse as well as to monitor the resulting tissue displacement. The tissue displacement response is directly related to the magnitude of the applied force and inversely related to the tissue stiffness. By sequentially interrogating different beam lines with focused radiation force and then synthesizing an image from the tissue response at a given time after the push (typically < 1 ms), as shown schematically in Figure 5, images of tissue displacement

green, areas of low strain (stiff tissue) in blue, and areas of high strain (soft tissue) in red. (b) Different color scale; red means stiff tissue. (c) Another type of display method is to show the elastogram in gray scale with B-mode images side-by-side. In this case, the location in the elastogram can be indicated on the B-mode display with a cursor.

	Score	Pattern	Elastogram	B-mode	
Benign	1				Entire hypoechoic area is soft
	2				Part of hypoechoic area is hard
	3				Only inside of margin of hypoechoic area is soft
Malignant	4				Entire hypoechoic area is hard
	5				Hypoechoic area and surrounding area are hard
	BGR				In the case of cysts, a specific blue-green-red pattern (BGR sign) is seen

Figure 4. Elasticity score in breast cancer diagnosis. The elasticity score is a five-point scale used to classify elastography patterns from benign to malignant as follows: score 1 (benign), score 2 (probably benign), score 3 (benign or malignant are equivocal), score 4 (malignancy suspected), and score 5 (malignancy strongly suggested). In the case of cysts, a specific blue-green-red (or black-gray-white) pattern called the BGR sign is seen from the body surface side. This is a type of artifact, but because the level of the internal echo signals from a cyst is low, it can be used for cyst diagnosis, like a lateral shadow or posterior enhancement on B-mode images.

that portray relative differences in tissue stiffness are generated (Figure 6) with similar information to the images generated in strain imaging. This imaging approach is implemented as Siemens Virtual Touch™ Imaging (VTI).

Appropriate measurement conditions and artifacts in strain imaging

Many manufacturers provide elastography equipment employing strain elastography, but the imaging methods differ slightly, as do the recommended measurement conditions. In terms of artifacts in strain elastography, it should be noted that the stress distribution is not uniform within the body and that tissue elasticity is nonlinear as explained in the next paragraph and in section 4.3.

An artifact resulting from non-uniform stress distribution is shown in Figure 7. In many cases, this type of artifact is easily recognized by *a priori* information such as the shape of the tumor. Artifacts due to the nonlinearity of tissue are also observed (Figure 8). The nonlinearity becomes marked when the compression generates strain in excess of several percent (i.e., for a typical breast of 3-cm thickness, a reading of 1.5 mm would be 5% strain). However, when strain of approximately 1% (i.e., 0.3 mm for a typical breast of 3-cm thickness) is generated in the mammary gland, stability and reproducibility can be achieved even if the level of compression fluctuates because it is within the linear range. Various available commercial systems have different image processing

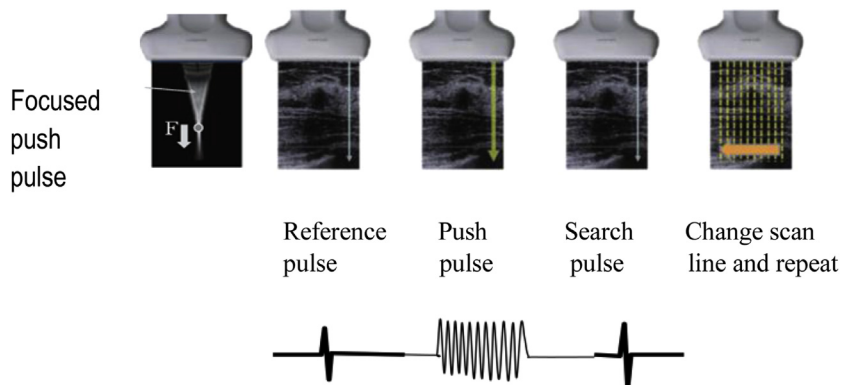


Figure 5. Pulse sequence in ARFI Imaging.

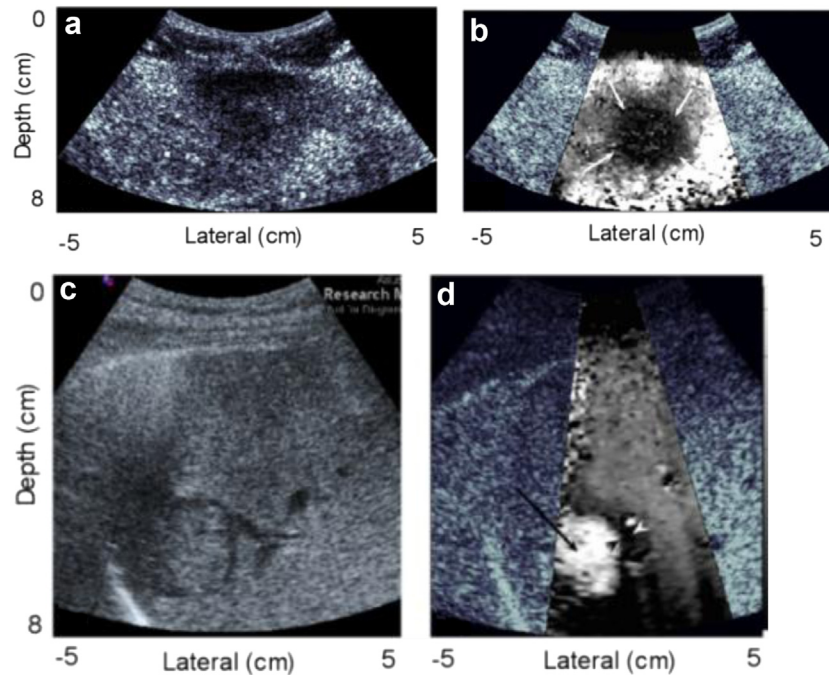


Figure 6. The top image pair shows a metastatic melanoma mass in an otherwise healthy liver. The mass appears as a hypoechoic region in the B-mode image; in the corresponding ARFI image, the malignant mass does not displace (darker region) as much as the background liver tissue (white) and can be interpreted to be stiffer than the liver tissue. The lower image pair shows B-mode and ARFI images of a hepatocellular carcinoma in a cirrhotic liver. In the ARFI image, the mass appears more compliant (i.e., displaces more) than the stiffer, diseased liver tissue. (Image reproduced and modified with permission from Physics in Medicine and Biology (Fahey et al., 2008)).

methods, and thus, they have different recommended methods for the magnitude of the applied compression, as well as the rate at which it should be applied.

ARFI imaging does not rely on transducer compression as the quasi-static strain elastography methods do, and thus, it has the advantage of being able to focus the 'push' within deep lying organs, where it can be difficult to generate deformation with compression from the body surface. However, as with strain elastography, nonlinear tissue responses can be generated by transducer compression, so minimal compression should be applied during ARFI imaging. In addition, the 'push' pulses are of longer duration than standard diagnostic pulses, and current methods typically employ relatively low frame rates to maintain acoustic output within diagnostic limits.

SHEAR WAVE SPEED MEASUREMENT AND IMAGING

Shear wave imaging methods monitor the propagation of shear waves in tissue. In contrast to ultrasonic or compressive waves that propagate in the same direction as the tissue displacement, shear waves propagate in a direction orthogonal to the direction of the tissue displacement (Table A1 in Appendix). These methods estimate the

speed of shear wave propagation (c_s) through tissues, which, assuming that tissue has very simple behaviors (i.e., linear, isotropic, and homogeneous), is related to the underlying material stiffness through Eq. (2) ($G = \rho c_s^2 = E/3$). As with strain imaging, shear waves can be generated from a variety of sources, including external vibration, physiologic motion, and acoustic radiation force, and in the research community, methods have been developed exploiting each of these. Tables 2a and 2b summarize the commercially available shear wave speed systems, including their methods of excitation and measurements reported, as described in the following sections.

Shear wave methods that use external sources

Two commercial methods employ external sources to induce shear waves. One uses ultrasound to monitor the shear wave propagation and is called Transient Elastography, as described below. The other employs magnetic resonance imaging to monitor shear wave propagation, called magnetic resonance elastography (MRE) (Mariappan, Glaser, & Ehman, 2010). Unlike all currently available ultrasound shear-wave elastography systems, which use shear-wave pulses, MRE tends to employ continuously vibrating sources. It should also be noted that MRE methods report images of shear modulus

($G = E/3$), whereas ultrasonic-based shear wave methods report either shear wave speed (c_s) or Young's modulus ($E = 3G = 3\rho c_s^2$), which are related through Eq. (2).

Transient Elastography. The first commercially available ultrasonic shear wave measurement system, FibroScan™ (Echosens, Paris, France), was based upon the concept of transient elastography (Sandrin *et al.*, 2003). This system employs a controlled external mechanical excitation (using a piston that 'punches' the body surface) that is integrated with an ultrasonic transducer to monitor the pulse of shear waves that is generated by the punch. The ultrasonic transducer has a fixed focal configuration, and the shear wave speed that is measured corresponds to the average shear wave speed in the region of tissue along the 'A-line' that is imaged by the transducer. The FibroScan™ displays the corresponding Young's modulus, computed using Eq. (2), and is specifically designed for measuring liver stiffness without displaying a B-mode image.

Acoustic Radiation Force shear wave methods

In acoustic radiation force-based shear wave methods, a focused acoustic beam is used to generate

shear waves via an acoustic radiation force impulse, and ultrasonic imaging is used to monitor the resulting shear wave propagation away from the radiation force 'push' location. B-mode image guidance is possible during the measurement because the same transducer is used to generate the shear waves and to image its propagation. As shown in Tables 2a and 2b, methods have been developed that provide 'point' measurements, reporting average shear wave speed (and/or Young's modulus) in a local region of interest, as well as 2D images that portray shear wave speed (and/or Young's modulus) at rates of up to a few frames per second.

What is Acoustic Radiation Force? Acoustic radiation force results from a transfer of momentum from the propagating ultrasonic wave to the tissue through which it is propagating due to absorption and scattering mechanisms. The magnitude of the applied acoustic radiation force (F) can be related to the acoustic absorption (α) and speed of sound (c) in the tissue and the temporal average intensity of the acoustic beam (I) by (Nyborg, Litovitz, & Davis, 1965; Torr, 1984):

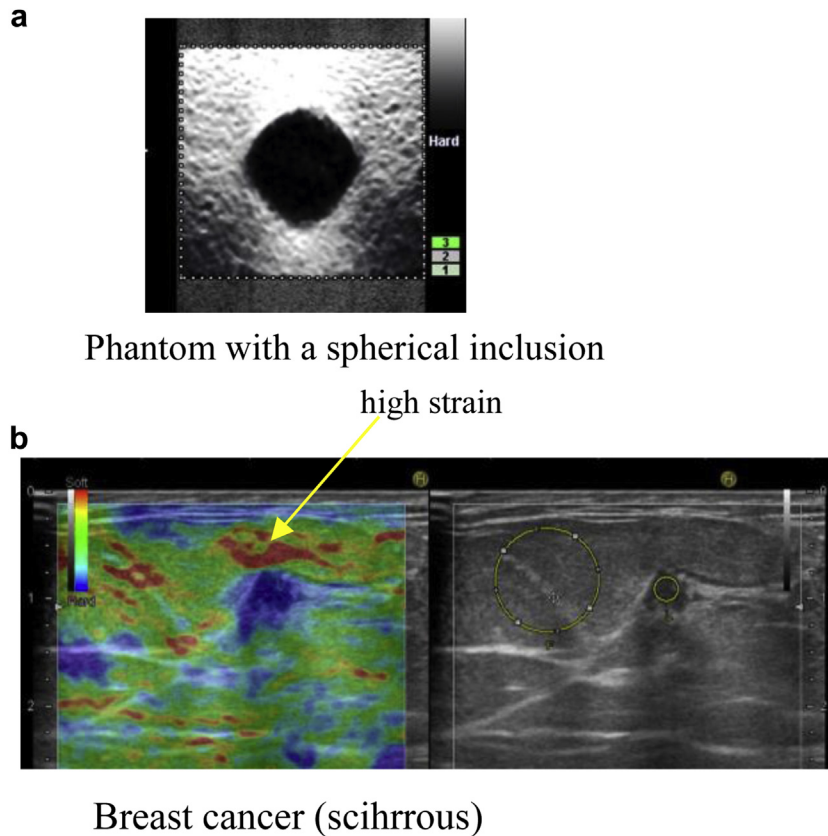


Figure 7. Artifacts due to stress concentration. Strain is used as the index of stiffness instead of Young's modulus on the assumption that stress is uniform based on Eq. (1). However, in practice, stress tends to concentrate on curved boundaries so that strain increases along a boundary compared with the adjacent area. This phenomenon causes artifacts such that the region near the boundary looks softer than the adjacent area.

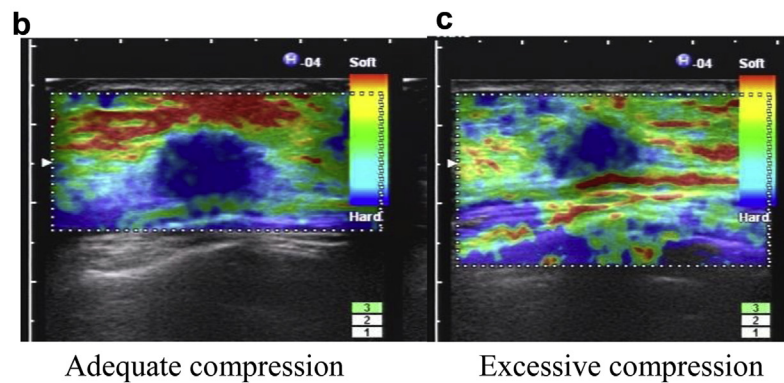
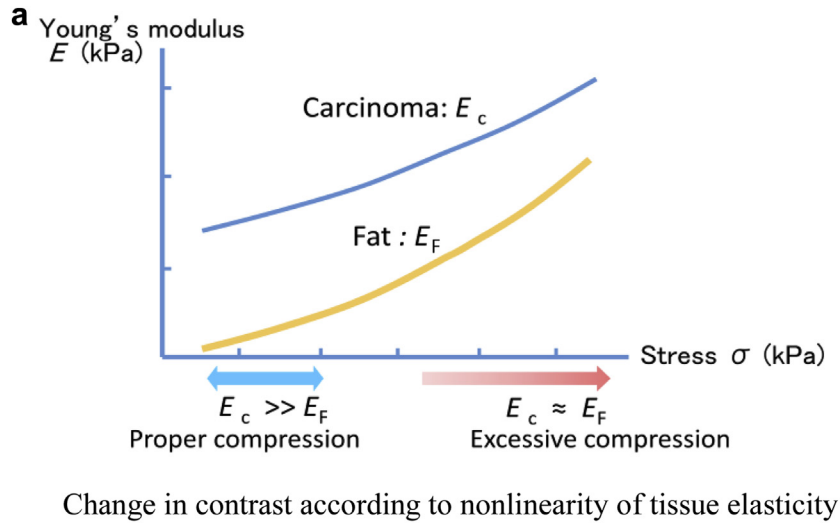


Figure 8. Nonlinearity of tissue elasticity and effect of excessive compression (breast cancer). In the case of biological tissue, when the compression is intensified, Young's modulus, i.e., stiffness, tends to increase and the contrast between fat and a malignant mass decreases as shown in (a). The extent of nonlinearity differs from tissue to tissue (Barr and Zhang 2012). For example, when the degree of compression is slight, the difference in Young's modulus between breast tissue and tumor is large, and the tumor is clearly displayed as a relatively low strain region, as shown in (b), but when the compression is too strong, the stiffness of the mammary gland increases, and the difference between it and the tumor will be smaller, possibly resulting in a false negative finding, as in (c). In the case of breast cancer diagnosis, one indicator is that the pectoralis major muscle is uniformly blue or black in grayscale (small strain) when elastography is performed with proper compression, but when the pectoralis major muscle is red, or white in grayscale (large strain) and the subcutaneous fat layer has blue (or black in grayscale) mixed in, it often means that excessive compression has been used.

$$F = \frac{2\alpha I}{c} \quad (4)$$

The transfer of momentum from the propagating acoustic wave to the tissue occurs over the duration of the acoustic pulse. In addition to vibrating at the ultrasonic frequency, the tissue within the region of excitation (ROE, or region where the ultrasound waves propagate and are absorbed) is deformed in response to a focused acoustic radiation force excitation, and shear waves propagate away from the ROE (Figure 9). While this phenomenon occurs with conventional B-mode imaging, the force magnitudes are too small to generate tissue motion that could be measured with conventional ultrasound. Through the use of longer duration acoustic pulses (0.05–1 ms) than are typically used in diagnostic ultrasound (< 0.02 ms),

transient soft tissue deformation on the order of microns (10^{-6} m) can be generated *in vivo*. Acoustic radiation force can be applied at a single focal location or a multiple focal zone configuration in which each focal zone is interrogated in rapid succession, leading to a cylindrically shaped shear wave extending over a larger depth, enabling real-time shear wave images to be formed. This multiple focal zone approach has been termed 'supersonic shear imaging' (SSI, J. Bercoff, Pernot, Tanter, & Fink, 2004).

Types of Displays. There is a tradeoff between precision and spatial resolution in shear wave speed estimation methods. The use of larger propagation distances to compute the wave speed presumes a larger homogeneous region and typically is associated with higher precision and accuracy; however, this comes at the expense of spatial

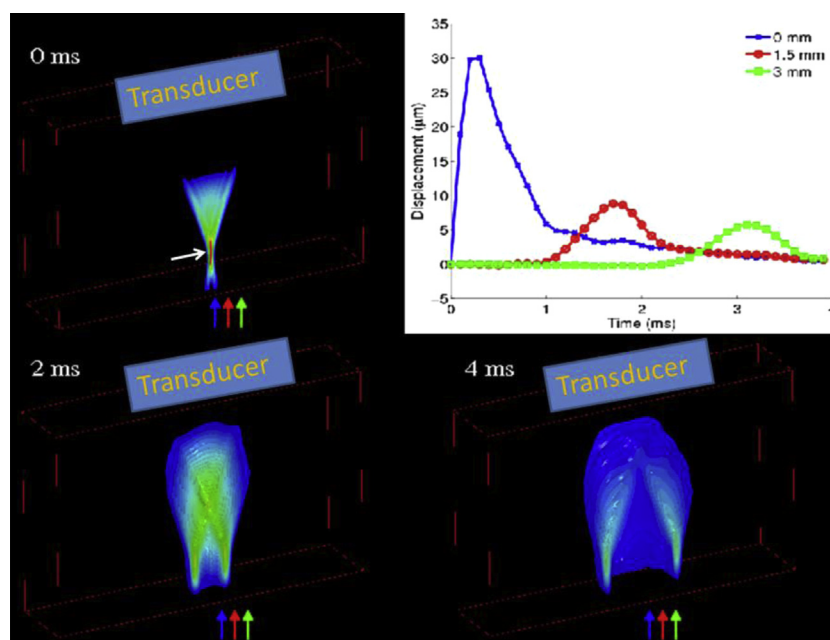


Figure 9. Examples of shear wave propagation represented as isocontours of displacement at different times after impulsive (i.e., < 1 ms) focused (white arrow) acoustic radiation force excitation. The 0 ms image reflects the force distribution in the region of excitation (ROE). The displacement amplitude is dictated by the underlying material stiffness, with more compliant materials displacing farther than stiffer materials. The ARFI images (Fig. 6) are generated by monitoring displacement along the central axis of the ROE, and translating the excitation throughout the imaging FOV. The plot in the upper right shows the displacement through time profiles at the focal depth of the radiation force excitation at three different lateral positions (indicated by the colored arrows in the isocontour images). Shear wave speed measurements are generated by monitoring the propagation between different lateral positions, as shown in the plot, where, for example, the wave arrives at 1.5 mm at 1.8 ms, and at 3 mm at 3.1 ms, so the wave speed is $(3 \text{ mm} - 1.5 \text{ mm}) / (3.1 \text{ ms} - 1.8 \text{ ms}) = 1.15 \text{ m/s}$.

resolution (Rouze *et al.*, 2012). Systems employing this approach are listed as ‘point measures’ in Table 2a,b. To generate two-dimensional shear wave images, smaller propagation distances are utilized to obtain better spatial resolution; however, decreasing the distance over which the shear wave is monitored increases the variance of the estimate at each pixel. Resolution of 1-2 mm has been reported for shear wave imaging systems (Defieux *et al.* 2009; McLaughlin & Renzi, 2006). Examples of point measurement and imaging approaches are shown in Figure 10.

Safety of Acoustic Radiation Force Imaging Methods. The safety of diagnostic ultrasonic imaging methods is monitored through several metrics, including Thermal Index (TI) related to the expected tissue heating and Mechanical Index (MI) related to the potential for inducing acoustic cavitation (i.e., rapid and violent collapse of a bubble which can be associated with highly localized tissue damage) (Meltzer, 1996). Acoustic radiation force-based imaging methods typically employ excitation pulses with similar pulse amplitudes ($1.0 < MI < 1.9$) and longer pulse durations (several hundred cycles) than those commonly used for diagnostic imaging (10-20 cycles for Doppler methods). Commercially avail-

able radiation force-based systems are designed to operate within accepted diagnostic limits; thus, no detrimental bioeffects are anticipated with these methods and none have been reported to date.

There are some specific imaging scenarios wherein bioeffects have been reported for diagnostic ultrasound, and given the longer pulse durations used in ARFI pulses, bioeffects would be anticipated, and possibly increased, in these cases. Application of the ALARA principle (Orenstein, 2011) would not likely support the use of ARFI imaging in these clinical scenarios until further bioeffects studies are performed. Reports of cavitation-based bioeffects have been associated with diagnostic ultrasound imaging in the presence of contrast agents and tissues known to contain gaseous bodies (e.g., lung) using MI values greater than 0.4 (Miller *et al.*, 2008)(Claudon *et al.*, 2013). Given that the MI values employed by acoustic radiation force excitation pulses are generally greater than 0.4 and approach 1.9 for liver imaging, it is likely that ultrasonic contrast agents would cavitate if exposed to these pulses. In addition, pulsed diagnostic ultrasound has been reported to increase fetal activity during exposure (Fatemi, Alizad, & Greenleaf, 2005), (Stratmeyer *et al.*, 2008), which has been postulated to be associated with

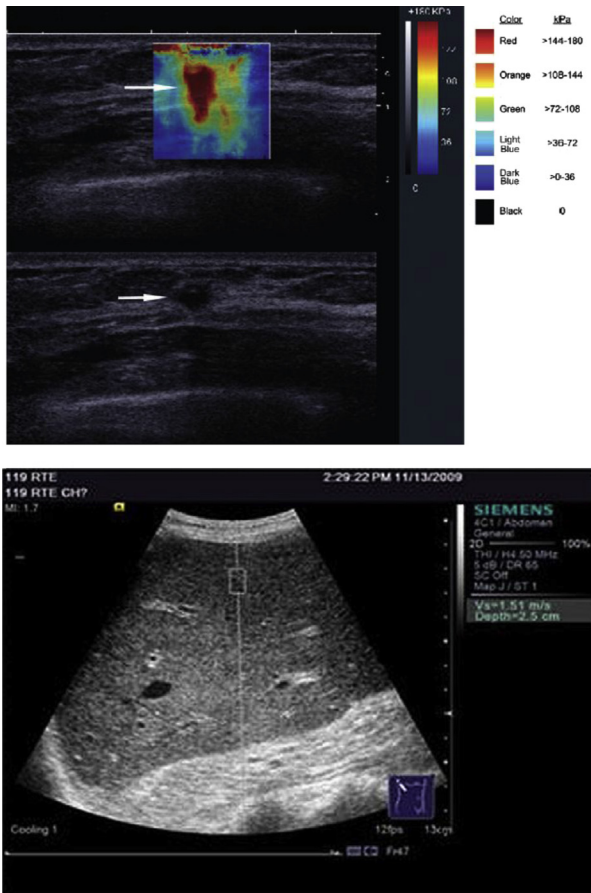


Figure 10. Example breast shear wave image (top) and corresponding BIRADS-5 B-mode image (middle) obtained with the SWETM method on an Aixplorer[®] system of a biopsy-confirmed infiltrating ductal carcinoma, which is very stiff ($E = 180$ kPa, or 7.7 m/s), making it highly suspicious for malignancy (reproduced from Berg et al., 2012). Example point measurement of local shear wave speed in a liver obtained with the VTTMQ (ARFI) method on an S2000[®] system (bottom) (image reproduced from Bota et al., 2012).

radiation force on the head or the inner ear, specifically the semicircular canals, in the audible frequency range (Fatemi et al., 2005). Although this bioeffect has not been shown to be detrimental, the radiation forces generated by ARFI pulses are applied using pulse durations 1-2 orders of magnitude longer than those associated with conventional B-mode/Doppler imaging and pre-clinical studies investigating the impact of ARFI-scale radiation forces on the fetus are needed to assess the ALARA principle for this application.

Appropriate measurement conditions and artifacts in shear wave speed measurement and imaging

While simplifying assumptions are employed in all of the systems listed in Tables 2a and 2b, soft tissues are known to be inherently nonlinear, viscoelastic,

and heterogeneous. These properties can affect the measurements. For example, adding viscosity to the tissue description (see appendix) means that the tissue stiffness and, thus, the shear wave speed, also depend on the excitation frequency, which is a phenomenon called dispersion. The effects of dispersion could result in differences between the measured shear wave speeds obtained with different commercial systems in a given patient.

Tissue material nonlinearities (e.g., hyperelastic material models) imply that the strain (ϵ) in response to an applied stress (e.g., transducer compression or acoustic radiation force) is dependent on the initial strain state of the material (i.e., the values reported by the systems can change with tissue compression). This phenomenon is described in the context of strain imaging in Figure 8, and it similarly impacts shear wave measurement systems. Increasing shear wave speeds have been correlated with increasing transducer compression during measurement in both breast and prostate tissues (Barr & Zhang, 2012). In addition, liver shear wave speed increases have been correlated with portal hypertension (Bureau et al., 2008), a phenomenon that has been shown to be associated with the nonlinear nature of hepatic tissue (Rotemberget al. 2012). The impact of neglecting this behavior is currently unclear; however, similar to strain imaging, application of minimal compression (e.g., < 0.3 mm in a typical 3 cm thick breast) during imaging is desirable to improve reproducibility.

When the assumption of tissue homogeneity within the shear wave estimation region is violated, artifacts can occur, leading to incorrect shear wave speed estimates. These artifacts arise from shear wave reflections at structural interfaces and can result in a ‘soft-center’ artifact in shear wave images of very stiff lesions (Deffieux et al. 2011; Rouze et al., 2012). This artifact is likely a contributing factor to the challenges reported in characterizing BIRADS-5 breast lesions with shear wave speed imaging (Berg et al., 2012). It is helpful to exclude structural boundaries that are visible on B-mode from the measurement region when using ‘point measurement’ systems.

The development of application-specific algorithms, standardization of imaging protocols, and calibration standards for shear wave imaging systems is underway through an international effort supported by the RSNA Quantitative Imaging Biomarker Alliance (Hall et al. 2013), with the goal of characterizing and minimizing the impact of these confounding effects.

RELATIONSHIP BETWEEN STRAIN, DISPLACEMENT, AND SHEAR WAVE SPEED

Strain, displacement, and shear wave speed images provide information related to the underlying tissue

stiffness. As such, in the absence of artifacts, correlation between these image types in a given patient is expected to be high. In general, strain images exhibit higher spatial resolution, and shear wave images have higher contrast; however, when the simplifying assumptions used to derive the images and measurements for different methods do not accurately reflect tissue behaviors, differences between images from different techniques can be anticipated. Tissue nonlinearity is associated with decreased elastogram contrast for some pathologies (Figure 8) and increased shear wave speeds with excessive transducer compression. As a result, for both strain and shear wave methods, minimizing the amount of transducer compression used during imaging (less than 1% or 0.3 mm for a typical 3-cm thickness breast) will result in the most reproducible imaging scenario. Tissue heterogeneities will also impact both approaches, leading to artifacts arising from the reflected waves in shear wave speed images and strain concentrations surrounding tissue heterogeneities. A more detailed investigation of the impact of these assumptions and associated image artifacts should be carried out in the future.

CONCLUSION

Tissue elasticity imaging and measurement provide the opportunity to improve the value of ultrasonography by combining the characteristic features of ultrasound, i.e., noninvasiveness, real-time capability, and ease of use, with the ability to provide new diagnostic information on the elastic properties of tissues. The first commercial equipment for elastography was released in 2003, but today most manufacturers offer an elastography option, and some manufacturers offer both strain and shear wave-based approaches. This could be considered a testament to the utility of elasticity imaging. On the other hand, it is still an evolving technology with much technical potential for clinical application in the future, including expanding its scope of quantification, 3D measurement, and treatment support. One might anticipate that it will continue to evolve in the future and will attain a position equal to that of Doppler as a new mode of ultrasound imaging.

Questions and Answers

1. What is the difference between *point shear wave speed measurement* and *shear wave speed imaging*?

Point shear wave speed measurement provides an average measurement of stiffness from a localized region of tissue indicated by the size and position of the ROI box, which should be positioned in a homogeneous region of tissue, away from structural boundaries. Shear wave speed imaging generates a 2D image of stiffness over a larger region of tissue, and generally with improved res-

olution, but with decreased precision at each image pixel. The resolution of a shear wave image may, of course, be sacrificed to improve precision by averaging the data within an analysis ROI box.

2. How is the *Young's modulus, E, (kPa)* related to the *shear wave speed, c_s , (m/s)* when reported by commercially available shear wave imaging systems?

$E = 3c_s^2$ (under certain limiting assumptions, which may include neglecting structural stiffness). Note that MRE systems report *shear modulus, G, (kPa)*, related to the above as $G = c_s^2 = E/3$.

Acknowledgments—The authors acknowledge the cooperative contributions provided by the following companies: Echosens, Esaote, GE Healthcare, Hitachi Aloka Medical, Philips, Siemens Healthcare, Supersonic Imagine, and Toshiba Medical Systems. Furthermore, the authors gratefully acknowledge Glynis Harvey and Stephanie Hynes from the WFUMB office for their efficient management.

REFERENCES

- Bamber JC, Cosgrove D, Dietrich CF, Fromageau J, Bojunga J, Calliada F, Cantisani V, Correas J-M, D'Onofrio M, Drakonaki EE, Fink M, Friedrich-Rust M, Gilja OH, Havre RF, Jessen C, Klauser AS, Ohlinger R, Săftoiu A, Schaefer F, Sporea I, Piscaglia F. EFSUMB guidelines and recommendations on the clinical use of ultrasound elastography. Part 1: Basic principles and technology. *Ultraschall Med* 2013;34:169–184.
- Bamber JC. Ultrasound elasticity imaging: definition and technology. *European Radiology* 1999;9:S327–S330.
- Bamber JC, Bush NL. Freehand elasticity imaging using speckle decorrelation rate. *Acoust Imaging* 1996;22:285–292.
- Bamber JC, Barbone PE, Bush NL, Cosgrove DO, Doyely MM, Fueschsel FG, Meaney PM, Miller NR, Shiina T, Tranquart F. Progress in freehand elastography of the breast. *IEICE Trans Inf Syst* 2002;E85D:5–14.
- Barbone PE, Gokhale NH. Elastic modulus imaging: on the uniqueness and nonuniqueness of the elastography inverse problem in two dimensions. *Inverse Probl* 2004;20:283–296.
- Barr RG, Zhang Z. Effects of precompression on elasticity imaging of the breast - development of a clinically useful semiquantitative method of precompression assessment. *J Ultrasound Med* 2012; 31:895–902.
- Bercoff JJ, Tanter M, Fink M. Supersonic shear imaging: a new technique for soft tissue elasticity mapping. *IEEE Trans Ultrason Ferroelectr Freq Control* 2004;51:396–409.
- Bercoff J, Pernot M, Tanter M, Fink M. Monitoring thermally-induced lesions with supersonic shear imaging. *Ultrasonic Imaging* 2004; 26:71–84.
- Berg WA, Cosgrove DO, Doré CJ, Schäfer FKW, Svensson WE, Hooley RJ, Ohlinger R, Mednelson EB, Balu-Maestro C, Locatelli M, Tourasse C, Cavanaugh BC, Juhani V, Stavros T, Tardivon A, Gay J, Henry JP, Cohen-Bacrie C. Shear-wave elastography improves the specificity of breast US: the BE1 study of 939 masses. *Radiology* 2012;262:435–449.
- Bureau C, Metivier S, Peron JM, Selves J, Robic MA, Gourraud PA, Rouquet O, Dupuis E, Alric L, Vinel JP. Transient elastography accurately predicts presence of significant portal hypertension in patients with chronic liver disease. *Alimentary Pharmacology and Therapeutics* 2008;27:1261–1268.
- Chen SG, Fatemi M, Greenleaf JF. Quantifying elasticity and viscosity from measurement of shear wave speed dispersion. *J Acoust Soc Am* 2004;115:2781–2785.
- Claudon M, Dietrich CF, Choi BI, Cosgrove DO, Kudo M, Nolsøe CP, Piscaglia F, Wilson SR, Barr RG, Chammas MC, Chaubal NG, Chen M-H, Clevert DA, Correas JM, Ding H, Forsberg F, Fowlkes JB, Gibson RN, Goldberg BB, Lassau N, Leen ELS, Mattrey R, Moriyasu F, Solbiati L, Weskott H-P, Xu H-X. Guidelines

- and good clinical practice recommendations for contrast enhanced ultrasound (CEUS) in the liver - update 2012: A WFUMB-EFSUMB Initiative in Cooperation with Representatives of AFSUMB, AIUM, ASUM, FLAUS and ICUS. *Ultrasound Med Biol* 2013;39:187–210.
- Cosgrove D, Piscaglia F, Bamber J, Bojunga J, Correas J-M, Gilja OH, Klauser AS, Sporea I, Calliada F, Cantisani V, D'Onofrio M, Drakonaki EE, Fink M, Friedrich-Rust M, Fromageau J, Havre RF, Jenssen C, Ohlinger R, Săftoiu A, Schaefer F, Dietrich CF. EFSUMB guidelines and recommendations on the clinical use of ultrasound elastography. Part 2: Clinical applications. *Ultraschall Med* 2013;34:238–253.
- Deffieux T, Gennisson J-L, Bercoff J, Tanter M. On the effects of reflected waves in transient shear wave elastography. *IEEE Trans Ultrason Ferroelectr Freq Control* 2011;58:2032–2035.
- Deffieux T, Montaldo G, Tanter M, Fink M. Shear wave spectroscopy for in vivo quantification of human soft tissues visco-elasticity. *IEEE Trans Med Imaging* 2009;28:313–322.
- Doherty JR, Trahey GE, Nightingale KR, Palmeri ML. Acoustic radiation force elasticity imaging in diagnostic ultrasound. *IEEE Trans Ultrason Ferroelectr Freq Control* 2013;60:685–701.
- Duck FA. *Physical properties of tissues*. New York: Academic press; 1990.
- Fahey BJ, Nelson RC, Bradway DP, Hsu SJ, Dumont DM, Trahey GE. In vivo visualization of abdominal malignancies with acoustic radiation force elastography. *Phys Med Biol* 2008;53:279–293.
- Farrokh A, Wojcinski S, Degenhardt F. Diagnostic value of strain ratio measurement in the differentiation of malignant and benign breast lesions. *Ultraschall Med* 2011;32:400–405.
- Fatemi M, Alizad A, Greenleaf JF. Characteristics of the audio sound generated by ultrasound imaging systems. *J Acoust Soc Am* 2005;117:1448–1455.
- Fehrenbach J. Influence of Poisson's ratio on elastographic direct and inverse problems. *Phys Med Biol* 2007;52:707–716.
- Fung YC. *Biomechanics: mechanical properties of living tissues*. New York: Springer-Verlag; 1993.
- Garra BS, Cespedes EI, Ophir J, Spratt SR, Zuurbier RA, Magnan CM, Pennanen MF. Elastography of breast lesions: initial clinical results. *Radiology* 1997;202:79–86.
- Greenleaf JF, Fatemi M, Insana M. Selected methods for imaging elastic properties of biological tissues. *Annu Rev Biomed Eng* 2003;5:57–78.
- Hall TJ, Zhu YN, Spalding CS. In vivo real-time freehand palpation imaging. *Ultrasound Med Biol* 2003;29:427–435.
- Hall T, Milkowski A, Garra B, Carson P, Palmeri M, Nightingale N, Lynch T, Alturki A, Andre M, Audiere S, Bamber J, Barr R, Bercoff J, Bercoff J, Bernai M, Brum J, Chan HW, Chen S, Cohen-Bacrie C, Couade M, Daniels A, DeWall R, Dillman J, Ehman R, Franchi-Abella SF, Fromageau J, Gennisson J-L, Henry JP, Ivancevich N, Kalin J, Kohn S, Kugel J, Lee K, Liu NL, Loupas T, Mazernik J, McAleavey S, Miette V, Metz S, Morel BM, Nelson T, Nordberg E, Oudry J, Padwal M, Rouze N, Samir A, Sandrin L, Schaccitti J, Schmitt C, Shamdassani V, Song P, Switalski P, Wang M, Wear K, Xie H, Zhao H. RSNA/QIBA: shear wave speed as a biomarker for liver fibrosis staging. In: Saniie J, (ed). *International Ultrasonics Symposium Proceedings*. Piscataway, NJ: IEEE International; 2013. pp. 397–pp.400.
- Itoh A, Ueno E, Tohno E, Kamma H, Takahashi H, Shiina T, Yamakawa M, Matsumura T. Breast disease: clinical application of US elastography for diagnosis. *Radiology* 2006;239:341–350.
- Krouskop TA, Wheeler TM, Kallel F, Garra BS, Hall TJ. The elastic moduli of breast and prostate tissues under compression. *Ultrason Imaging* 1998;20:260–274.
- Manduca A, Oliphant TE, Dresner MA, Mahowald JL, Kruse SA, Amromin E, Felmlee JP, Greenleaf JF, Ehman RL. Magnetic resonance elastography: non-invasive mapping of tissue elasticity. *Medical Image Analysis* 2001;5:237–254.
- Mariappan YK, Glaser KJ, Ehman RL. Magnetic resonance elastography: a review. *Clinical Anatomy* 2010;23:497–511.
- Matsumura T, Umemoto T, Fujihara Y, Ueno E, Yamakawa M, Shiina T, Mitake T. Measurement of elastic property of breast tissue for elasticity imaging. In: Yuhus MP, (ed). *Ultrasonics Symposium (IUS)*. Piscataway, NJ: IEEE International; 2009. pp. 1451–1454.
- McLaughlin J, Renzi D. Shear wave speed recovery in transient elastography and supersonic imaging using propagating fronts. *Inverse Problems* 2006;22:707–725.
- Meltzer RS. Food and Drug Administration ultrasound device regulation: The output display standard, the “mechanical index,” and ultrasound safety. *Journal of the American Society of Echocardiography* 1996;9:216–220.
- Miller DL, Averkiou MA, Brayman AA, Everbach EC, Holland CK, Wible J, Wu J. Bioeffects considerations for diagnostic ultrasound contrast agents. *J Ultrasound Med* 2008;27:611–632.
- Morikawa H, Fukuda K, Kobayashi S, Fujii H, Iwai S, Enomoto M, Tamori A, Sakaguchi H, Kawada N. Real-time tissue elastography as a tool for the noninvasive assessment of liver stiffness in patients with chronic hepatitis C. *J Gastroenterol* 2011;46:350–358.
- Nightingale K, Palmeri M, Nightingale R, Trahey G. On the feasibility of remote palpation using acoustic radiation force. *The Journal of the Acoustical Society of America* 2001;110:625.
- Nightingale KR, McAleavey SA, Trahey GE. Shear-wave generation using acoustic radiation force: in vivo and ex vivo results. *Ultrasound Med Biol* 2003;29:1715–1723.
- Nightingale KR, Soo MS, Nightingale RW, Trahey GE. Acoustic radiation force impulse imaging: in vivo demonstration of clinical feasibility. *Ultrasound Med Biol* 2002;28(2):227–235.
- Nyborg WLM, Litovitz T, Davis C. Acoustic streaming. In: Mason WP, (ed). *Physical acoustics Vol IIA*. New York, NY: Academic Press; 1965. pp. 265–331.
- Ophir J, Cespedes I, Ponnekanti H, Yazdi Y, Li X. Elastography: a quantitative method for imaging the elasticity of biological tissues. *Ultrasound Imaging* 1991;13:111–134.
- Oliphant TE, Manduca A, Ehman RL, Greenleaf JF. Complex-valued stiffness reconstruction for magnetic resonance elastography by algebraic inversion of the differential equation. *Magn Reson Med* 2001;45:299–310.
- Orenstein B. The ALARA principle and sonography. *Radiology Today* 2011;12:10.
- Parker KJ, Doyle MM, Rubens DJ. Imaging the elastic properties of tissue: the 20 year perspective. *Phys Med Biol* 2011;56:R1–R29.
- Parker KJ, Huang SR, Musulin RA. Tissue response to mechanical vibrations for sonoelasticity imaging. *Ultrasound Med Biol* 1990;16:241–246.
- Parker KJ, Taylor LS, Gracowski S, Rubens DJ. A unified view of imaging the elastic properties of tissue. *J Acoust Soc Am* 2005;117:2705–2712.
- Rotemberg V, Palmeri M, Nightingale R, Rouze N, Nightingale K. The impact of hepatic pressurization on liver shear wave speed estimates in constrained versus unconstrained conditions. *Phys Med Biol* 2012;57:329–341.
- Rouze NC, Wang MH, Palmeri ML, Nightingale KR. Parameters affecting the resolution and accuracy of 2-D quantitative shear wave images. *IEEE Trans Ultrason Ferroelectr Freq Control* 2012;59:1729–1740.
- Saada AS. *Elasticity theory and applications*. Malabar, FL: Krieger Publishing Company; 1993.
- Samani A, Zubovits J, Plewes D. Elastic moduli of normal and pathological human breast tissues: an inversion-technique-based investigation of 169 samples. *Phys Med Biol* 2007;52:1565–1576.
- Sandrin L, Fourquet B, Hasquenoph J-M, Yon S, Fournier C, Mal F, Christidis C, Ziol M, Poulet B, Kazemi F, Beaupre M, Palau R. Transient elastography: a new noninvasive method for assessment of hepatic fibrosis. *Ultrasound Med. Biol* 2003;29:1705–1713.
- Sarvazyan A, Rudenko O, Swanson S, Fowlkes JB, Emelianov SY. Shear wave elasticity imaging: a new ultrasonic technology of medical diagnostics. *Ultrasound Med Biol* 1998;24:1419–1435.
- Sarvazyan AP. Elastic properties of soft tissues. In: Levy, vass and stern, eds. *Handbook of elastic properties of solids, liquids and gases*. New York, NY: Academic Press; 2001. pp. 107–127.
- Sarvazyan A, Hill CR. Physical chemistry of the ultrasound-tissue interaction. In: Hill CR, Bamber JC, ter Haar GR, (eds). *Physical principles of medical ultrasonics*. Chichester: John Wiley; 2004. pp. 223–235.

- Shiina T, Doyley MM, Bamber JC. Strain imaging using combined RF and envelope autocorrelation processing. In: Levy M, Schneider SC, McAvor BR, (eds). International Ultrasonics Symposium Proceedings. Piscataway, NJ: IEEE International; 1996. pp. 1331–1336.
- Shiina T, Nitta N, Ueno E, Bamber JC. Real time elasticity imaging using the combined autocorrelation method. *J Med Ultrasonics* 2002; 29:119–128.
- Sinkus R, Lorenzen J, Schrader D, Lorenzen M, Dargatz M, Holz D. High-resolution tensor MR elastography for breast tumour detection. *Phys Med Biol* 2000;45:1649–1664.
- Sinkus R, Tanter M, Xydeas T, Catheline S, Bercoff J, Fink M. Viscoelastic shear properties of in vivo breast lesions measured by MR elastography. *Magn Reson Imaging* 2005;23:159–165.
- Stratmeyer ME, Greenleaf JF, Dalecki D, Salvesen KA. Fetal ultrasound mechanical effects. *J Ultrasound Med* 2008;27:597–605.
- Thomas A, Warm M, Hoopmann M, Diekmann F, Fischer T. Tissue Doppler and strain imaging for evaluating tissue elasticity of breast lesions. *Acad Radiol* 2007;14:522–529.
- Torr GR. The acoustic radiation force. *Am J Phys* 1984;52:402–408.
- Ueno E, Umamoto T, Bando H, Tohno E, Waki K, Matsumura T. New quantitative method in breast elastography: fat lesion ratio (FLR). In: Proceedings of the Radiological Society of North America Scientific Assembly and Annual Meeting. Oak Brook, IL: Radiological Society of North America; 2007. pp. 697 (abstract).
- Varghese T, Ophir J. A theoretical framework for performance characterization of elastography: the strain filter. *IEEE Trans Ultrason Ferroelectr Freq Control* 1997;44:164–172.
- Wells PNT, Liang H-D. Medical ultrasound: imaging of soft tissue strain and elasticity. *J R Soc Interface* 2011;8:1521–1549.

GLOSSARY

acoustic radiation force

- A physical phenomenon resulting from the interaction of an acoustic wave with the medium through which it is propagating, generated by a transfer of momentum from the wave to the medium, arising from the absorption and/or scattering/reflection of acoustic energy; the term ‘acoustic radiation’ refers to the propagation of acoustic energy, which is a form of non-ionizing radiation.

acoustic radiation force impulse (ARFI)

- A temporally impulse-like (i.e., very short duration, < 1 msec) acoustic radiation force, typically generated with a focused acoustic beam. In the technical literature, this term has been used interchangeably with ‘ARFI imaging’, however, in the clinical and commercial product literature, this term has been used to refer to both ARFI imaging and quantitative ARFI.

acoustic radiation pressure

- The acoustic radiation force exerted on the surface of an object placed in the path of a propagating acoustic wave.

ARFI imaging

- A form of elasticity imaging that uses acoustic radiation force impulse (ARFI) excitation, and generates images related to the corresponding tissue displacement within the ARFI excitation beam. ARFI excitations are used to sequentially interrogate adjacent lateral positions within a specified field of view, with the corresponding images reflecting relative tis-

sue displacement. The information in these images is similar to that from strain images generated with external compression

ARFI quantification

- A term widely used in the clinical literature to describe the point shear wave elastography method employed by the Siemens VTTMQ feature. See also point shear wave elastography

axial strain

- Strain in the direction of the applied force. In elastography, this is generally in the direction of the acoustic beam, or the depth direction.

bulk modulus

- A fundamental material property that quantifies the resistance to volume change with increasing pressure. It is equivalent to the resistance to increase density with increasing pressure. The bulk modulus is the inverse of compressibility.

compressibility

- A measure of the relative volume change in response to a pressure change. Compressibility is the inverse of the bulk modulus. Note that there is a distinction between adiabatic (constant entropy) compressibility and isothermal (constant temperature) compressibility, but the distinction is beyond the scope of most needs in elastography.

compressional wave

- A mechanical wave that propagates in the direction of the particle displacement. A compressional wave is a propagating increase (and then decrease) in the local pressure or density. These are also known as acoustic waves, sound waves, pressure waves, p-waves or longitudinal waves.

dispersion (acoustics)

- The phenomena of a wave separating into its frequency components as it propagates. Dispersion is caused by the phase velocity in the material being frequency-dependent (generally, higher frequency component of the wave traveling faster than lower frequency components).

dispersive medium

- A material that exhibits dispersion.

elastic modulus

- A quantity relating the ability of a material to resist deformation when a force is applied. There are many elastic moduli that are specific to the type of force (or stress) and the type of deformation (or strain); see, for example, bulk modulus, shear modulus, Young’s modulus, and Poisson’s ratio.

elastic nonlinearity

- The increase in the slope of the stress-strain curve with increasing strain. It is a measure of the increased stiffness of a material as the deformation of that material increases.

elastogram

- An image of the (visco-) elastic properties of tissue.

elastography

- Any imaging method that provides information related to the stiffness (or another elastic property) of tissue.

group velocity

- The velocity at which the overall shape (modulation, envelope) of a wave propagates. It is the wave speed associated with the weighted sum of the individual phase velocities comprising the wave.

indentation test

- A method for estimating the mechanical properties of a material. Specifically, indentation tests are designed to measure the “hardness” of a material (generally, its ability to resist plastic deformation or fracture). This approach is sometimes used to estimate the Young’s modulus of a material.

kilopascal

- One thousand Pascals (kPa).

loss modulus

- The quantity describing inelastic (or viscous) response of a viscoelastic material to an applied force (stress). The loss modulus combines with the storage modulus (the elastic response or stored energy) to express the complex modulus.

magnetic resonance elastography (MRE)

- An elasticity imaging method that uses an external vibration device to generate shear waves, and Magnetic Resonance Imaging to monitor the tissue response to generate images of shear modulus (which is related to Young’s modulus by a factor of 1/3 under certain simplifying assumptions).

modulus of rigidity

- See shear modulus.

pascal

- A unit measure of pressure, stress, shear modulus, Young’s modulus or tensile strength. Named for the French mathematician and physicist Blaise Pascal, one pascal (Pa) is equivalent to one newton per square meter, and 1 kPa is approximately 0.01 atmospheres.

phase velocity

- The rate at which the phase of a wave, or any single frequency component of the wave, travels in space. The phase velocity is the ratio of the wavelength to the period of the wave.

point shear wave elastography

- An elasticity estimation method that generates a shear wave with acoustic radiation force, and reports a quantitative stiffness metric (either shear wave speed or Young’s modulus) that represents the average of that metric within a local region of interest that is assumed to be homogeneous.

Poisson’s ratio

- A fundamental material property that quantifies the negative ratio of transverse strain to longitudinal strain in an elastic material. For isotropic materials, Poisson’s ratio lies between -1 and 0.5. Incompressible materials have a Poisson’s ratio of 0.5. Named after the French mathematician and physicist Siméon Denis Poisson, Poisson’s ratio, like the shear modulus, describes the resistance of a material to changes in shape, but Poisson’s ratio relates a change in dimension in the direction of the applied load to the change in shape of the material in the perpendicular direction.

quasi-static loading

- The application of stress that happens sufficiently slowly such that the inertial effects are negligible (time dependence of the load and inertial mass can be ignored). This is in contrast to dynamic loading.

radiation force

- See acoustic radiation force.

shear modulus

- A material property that quantifies the resistance of a material to change its shape in shear (deformation of a material in which parallel internal surfaces slide past one another). It is defined as the ratio of the shear stress to the shear strain and is also known as the modulus of rigidity. The units of the shear modulus are Pascals.

shear strain

- The deformation of a body in which a cross sectional plane through the body is displaced parallel to itself. Such a deformation is the result of a shear stress.

shear stress

- The component of stress on a surface that is tangential to the surface. For flat surfaces, the force vector is in the plane of the surface. The units of shear stress are Pascals.

shear viscosity

- The resistance of a fluid to deformation (flow). A fluid with no viscosity is called an ‘ideal fluid’. Fluids that flow readily, such as water, are low viscosity. Fluids that resist flow, such as molasses, are high viscosity. The units of viscosity are Pascal – second.

shear wave

- A mechanical wave that propagates in the direction perpendicular to the particle displacement in an infinite material. These are a special type of transverse waves and are also known as s-waves.

shear wave elastography

- An elasticity imaging method that uses acoustic radiation force to generate shear waves and generates quantitative images of a stiffness metric (where the color bar represents either Young’s modulus or shear wave speed).

shear wave imaging

- An elastography method that induces and monitors shear wave propagation in tissue and reports a quantitative value related to the stiffness (i.e., shear wave speed, Young's modulus, shear modulus).

SNR (signal to noise ratio)

- The ratio of the amount of signal divided by the amount of noise present in data.

stiffness

- The extent to which an object resists deformation in response to an applied force.

strain

- A measure of relative deformation. The most commonly used form is referred to as "infinitesimal strain" or "engineering strain," which is the ratio of the total deformation (ΔL) divided by the initial dimension of the material (L), so that strain = $\Delta L/L$.

strain imaging

- An elastography method that generates images of tissue strain, which is related to both the structural stiffness of the object and the shear modulus of tissue.

stress

- The force per unit area acting on a body. Stresses can result from forces on the surface of the body or can be due to an internal particle (volume element) acting on an adjacent particle (volume element). The units of stress are the Pascal. See also particular types of stress such as compressive stress, shear stress and uniaxial stress.

stress concentration

- Localized stress that is considerably higher than the average surrounding stress. This is usually caused by an irregular surface shape or a local inclusion with different viscoelastic properties.

stress decay

- A loss in stress in an object either with time (such as in a stress relaxation experiment) or in space (such as due to diffraction effects from a surface indenter).

structural stiffness

- Stiffness arising from the structure of an object; an object's stiffness arises from both its shear modulus and the effect of its structure. For example, a thin membrane will have a lower structural stiffness and, hence, lower stiffness, than a thicker membrane of the same shear modulus, or a tube formed from a sheet of paper is stiffer than the sheet of paper due to the differences in structural stiffness.

transient elastography

- An elasticity estimation method that generates a shear wave with an external vibration and reports a quantitative stiffness metric (Young's modulus) that represents the average of that metric within a local region that is assumed to be homogeneous.

transverse strain

- That component of strain perpendicular to some relevant axis of the material.

transverse wave

- A wave that propagates in a direction that is perpendicular to the particle displacement.

uniaxial strain

- An idealized condition in which a planar surface (or cross section through a material) has uniform displacement perpendicular to the plane of the surface (or cross section).

uniaxial stress

- An idealized condition in which a planar surface (or cross section through a material) has uniformly distributed force over the entire surface and that force is perpendicular to the plane of the surface (or cross section).

viscoelastic material

- A material, such as a polymer or tissue, that is not perfectly elastic. A perfectly elastic material stores all energy from a deformation and releases that energy (such as to return to its initial state) when the applied force is removed. When a dynamic load is applied to a perfectly elastic material, the strain is in phase with the stress. For a purely viscous fluid, the strain will lag the stress by 90 degrees. A viscoelastic material will respond somewhere between these ideal cases.

viscosity

- See shear viscosity.

wave

- A disturbance or oscillation that travels through a medium.

Young's modulus

- A material property that indicates how difficult it is to deform a material by stretching or compression. It is the ratio of the uniaxial stress to the uniaxial strain (either compressive or tensile loading).

APPENDIX

This appendix provides a more in depth, although brief, description of the technical details related to tissue biomechanics and elasticity imaging. For thorough reviews of elasticity imaging methods, the reader is referred to the following review articles: (Duck 1990; Fung 1993; Saada 1993; Sarvazyan 2004; Sarvazyan 2001; Wells & Liang, 2011; Doherty et al. 2013); (Greenleaf, Fatemi, & Insana, 2003; Parker et al., 2005).

A.1 – Tissue Biomechanics

Stiffness is resistance to deformation, and application of external force is required to measure it. The behavior exhibited when a force is applied to the tissue is described as a **viscoelastic body** with **viscosity** and **elasticity**, and it can be approximated using the model shown in [Figure A1](#). As shown in [Figure A1\(a\)](#), the **stress** σ (equal to external force per unit area) and **strain** ϵ (equal to expansion per unit length)

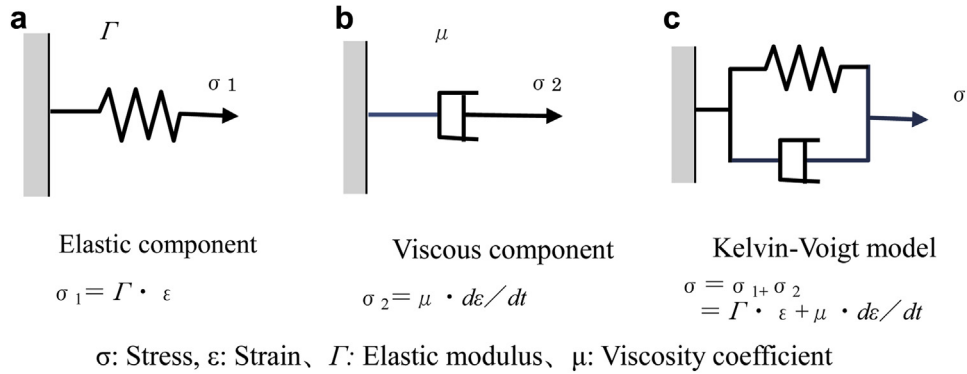


Figure A1. Viscoelastic model.

exhibit proportionality, which is known in Hooke’s law in Eq. (A1), and its coefficient is **elastic modulus** Γ .

$$\sigma_1 = \Gamma \cdot \varepsilon \tag{A1}$$

As shown in Figure A1 (b), as for the viscosity component, stress σ_2 is proportional to the speed of deformation, i.e., strain rate $d\varepsilon/dt$, and its coefficient μ is the **viscosity coefficient**.

$$\sigma_2 = \mu \frac{d\varepsilon}{dt} \tag{A2}$$

The mechanical characteristics of general tissue consist of a complex combination of elastic and viscous components, which are often approximated using a simplified model such as the one in Figure A1 (c). Where the speed of the applied external force is slow (such as manual compression), and the effect of viscosity can be disregarded in Eq. (A2), the model shown in Figure A1 (c) can approximate the dynamic properties with only the elastic component Figure A1 (a). Conversely, if high-frequency vibration is applied, the viscous component will have a major effect, the extent of which will depend on the frequency.

With regard to elasticity, three types of elastic moduli (Young’s modulus, shear modulus, and bulk modulus) are defined based on the method of deformation. **Young’s modulus** E is defined by the following equation when stress is applied longitudinally to a long, thin cylindrical object, and strain occurs as shown in Figure 2(a).

$$\sigma = E \cdot \varepsilon_L \tag{A3}$$

where σ is stress and $\varepsilon_L = \Delta L/L$ is (longitudinal) strain.

In the absence of volume change, a cylindrical object becomes thinner when stretched in Figure A2 (a). The percent change in the radial direction, $\varepsilon_r = \Delta r / r$, is called transverse strain, and the ratio of longitudinal strain to transverse strain,

$$\nu = \frac{\varepsilon_r}{\varepsilon_L} \tag{A4}$$

is called **Poisson’s ratio**. Poisson’s ratio indicates the extent of volume change caused by deformation, and ν is no higher than 0.5 in the case of an incompressible medium.

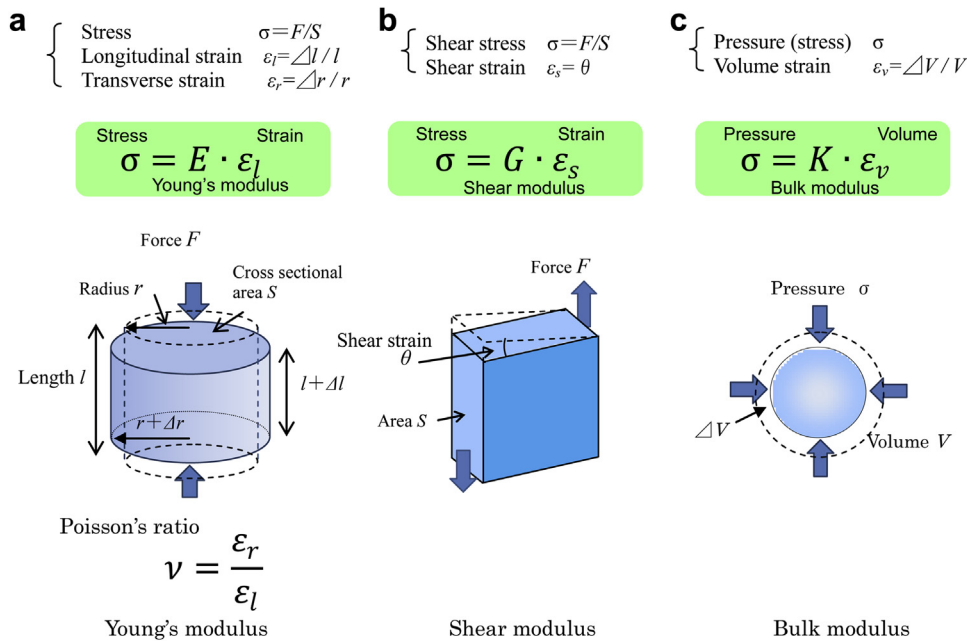


Figure A2. Various elastic moduli.

Shear modulus G is defined by the following equation for the shear deformation shown in [Figure A2](#) (b).

$$\sigma = G \cdot \varepsilon_s \tag{A5}$$

where $\varepsilon_s = \theta$ is shear strain.

Bulk modulus K is defined by the following equation when the volume changes under pressure.

$$\sigma = K \cdot \varepsilon_v \tag{A6}$$

where $\varepsilon_v = \Delta V/V$ is the volume strain. The larger the elastic modulus is, the smaller the strain will be with the same stress, so the object will be stiffer. For example, Young's modulus E is expressed as in Eq. (A7) using shear modulus G and Poisson's ratio ν . The water content of soft tissue is high, and consequently, its Poisson's ratio is near 0.5 of an incompressible medium, so Young's modulus will be equal to approximately three times the shear modulus, as in the following equation.

$$E = 2(\nu+1)G \tag{A7}$$

$$\cong 3G$$

Thus, the elastic modulus is defined for static deformations, but it is also a component that determines the propagation velocity of waves. Wave propagation generally involves **longitudinal waves** and **transverse waves**, as shown in [Table A1](#). In the case of ordinary ultrasound images, longitudinal waves are used, and the speed c_L of the longitudinal waves is

$$c_L = \sqrt{\frac{K}{\rho}} \tag{A8}$$

where ρ indicates the density of the medium, which is approximately 1540 m/s in soft tissues. Using the shear modulus, the speed c_s of transverse waves is expressed as

$$c_s = \sqrt{\frac{G}{\rho}} \tag{A9}$$

which is approximately 1-10 m/s in soft tissues.

Equations (A8) and (A9) indicate that the larger K and G are, i.e., the stiffer the medium is, the faster the wave will propagate. In the case of soft tissue, the speed of a longitudinal wave is comparable to the sound speed in water ($c_L=1500$ m/s); this means that there is little difference in K between tissues. In contrast, transverse waves, which are often called **shear waves**, attenuate rapidly and disappear in the MHz ultrasound band, but attenuation is lower and they can propagate *in vivo* when the frequency is below 1 kHz. Moreover, their velocity is quite low ($c_s=1-10$ m/s) compared with longitudinal waves, so G is

low (1-100 kPa), and the difference between tissues is large, which enables elasticity imaging methods to reconstruct images with high tissue contrast ([Saravazyan et al. 2004](#)).

On the other hand, unlike static deformation, **velocity dispersion** caused by the viscosity occurs during wave propagation when the frequency is high in soft tissues. For example, when the Kelvin-Voigt model is used ([Figure A1](#) (c)), the following equation is derived for the speed of a transverse wave instead of Eq. (A9) as a result of taking viscosity into account ([Defieux et al. 2009](#)).

$$c_s = \sqrt{\frac{2\{G^2 + (2\pi\mu f)^2\}}{\rho\{G + \sqrt{G^2 + (2\pi\mu f)^2}\}}} \tag{A10}$$

Thus, shear wave speed becomes a function of frequency f , and the higher the frequency is, the faster the speed. This could lead to differences in shear wave speeds measured with different imaging systems, and the magnitude of this possible effect remains the focus of the QIBA work (RSNA, n.d.).

A.2 Ultrasonic displacement measurement

In strain imaging, displacement in the direction of pulse propagation is measured to calculate strain, while in shear wave speed imaging, the displacement of tissue in the direction perpendicular to the shear wave propagation is measured to calculate their speed. Thus, measurement of displacement is a key technology in all elastography techniques, and there are several methods for measuring it. As shown in [Table 2a](#), strain elastography is now installed in ultrasound equipment of many manufacturers; however, each manufacturer uses their own method for measuring displacement, which results in differences in image characteristics such as spatial and temporal resolution and differences in optimal measurement conditions.

The typical methods for measuring displacement are shown below.

(1) Spatial correlation method (speckle tracking method, pattern matching method)

This is a method that tracks the movement of image patterns. Because patterns move while maintaining their speckle pattern as long as the strain is extremely slight, in this method, the amount of movement, i.e., displacement, is sought by setting a region of interest (ROI) and calculating the spatial correlation of the ROI before and after compression.

The simplest method is to measure 1D displacement along the beam axis, as shown in [Figure A3](#) (a). The cross-correlation coefficient in Eq. (A11) is calculated to evaluate the degree of similarity. Calculation of the cross-correlation coefficient is repeated while moving the window, and displacement is defined as the amount of movement when the correlation is at its maximum.

Table A1. Longitudinal waves and transverse waves

	Direction of propagation and vibration	Sound speed	Main use (frequency)
Longitudinal wave (compression wave)		$c_L = \sqrt{\frac{K}{\rho}}$ K ~ 2 GPa Soft tissue $c_L \cong 1500$ m/s	Imaging by pulse-echo method (MHz band)
Transverse wave (shear wave)		$c_s = \sqrt{\frac{G}{\rho}}$ G = 1-100 kPa Soft tissue $c_s = 1-10$ m/s	Elastography (≤ 1 kHz)

C: Compression, R: Rarefaction

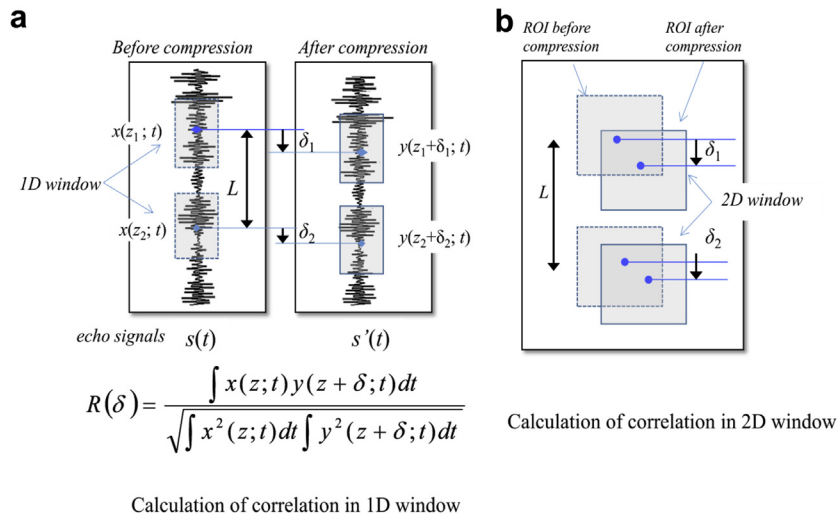


Figure A3. Calculation of correlation using the spatial correlation method.

$$R(\delta) = \frac{\int x(z; t)y(z + \delta; t)dt}{\sqrt{\int x^2(z; t)dt \int y^2(z + \delta; t)dt}} \quad (A11)$$

where, $x(z; t)$ and $y(z; t)$ are echo signals before and after compression, respectively, which are clipped out in the window centered around a depth z .

In reality, each ROI moves in the azimuth direction in the cross section. Therefore, an adjustment is made to estimate the displacement more accurately by performing a 2D search in both the range direction and the azimuth direction, as shown in Figure A3(b). In addition, tissue also moves in the slice direction, but the beam width in the slice direction is generally large when an ordinary electronic scanning probe is used, so the impact is smaller than in the azimuthal direction as long as the cross section does not deviate considerably.

(2) Phase difference detection method (Doppler method)

As shown in Figure A4, this is basically the same method as that used in color Doppler and tissue Doppler (Thomas et al. 2007). The phase difference between echo signals obtained by transmitting repeated pulses is detected by an autocorrelation method to calculate displacement.

As shown in Table A2, the advantages of the Doppler method are its excellent real-time capability and its relative robustness to noise, but only 1D displacement in the beam direction can be measured because of angle dependence, and errors occur from aliasing when measuring a large displacement that exceeds half the wavelength.

The advantages of the speckle tracking method are that it is possible to measure large displacements that exceed the wavelength,

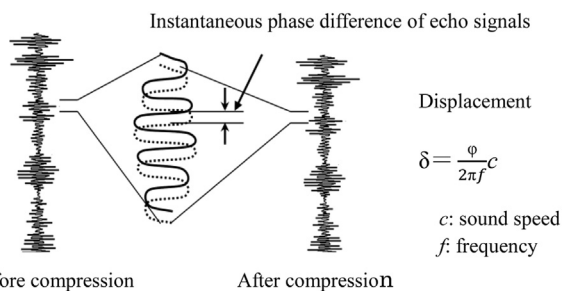


Figure A4. Measurement of displacement with the phase difference detection method.

provided the change in the speckle pattern is within a small range, and it is possible to track the movement of the ROI in 2D and 3D. However, the disadvantage is that the real-time capability may be lost as the calculation of correlation requires enormous computational power. In addition, it is susceptible to the effects of noise, and it is prone to detection errors when the speckle pattern is unclear because of weak echoes, etc.

(3) Combined method

From the standpoint of practical application in clinical settings, a high degree of accuracy to accommodate small displacements and a dynamic range wide enough to handle large displacements are necessary because fluctuations in the speed of compression are large when manual compression is used. In addition, deformation occurs not only in one dimension in the beam direction but also in the azimuthal direction because of the lateral deformation of tissue, etc. Moreover, in practice, the real-time capability is critical along with accuracy. Therefore, a combined autocorrelation method that combines the merits of the phase difference detection method and the spatial correlation method was developed (Shiina et al. 1996, 2002), as shown in Figure A5.

This combined method with the improved spatial correlation method and phase difference method have been implemented in current systems, but differences in their characteristics are manifested as differences in frame rate, image quality, and measurement conditions, etc.

A.3 Shear wave imaging

The first shear wave imaging methods to be developed employed external vibration to induce shear waves in tissues, with both ultrasonic (Sandrin et al., 2003) and MR imaging (Manduca et al., 2001; Sinkus et al., 2000a; Sinkus et al., 2005) methods used to monitor the wave propagation. Shear waves that are generated by acoustic radiation force, as shown in Figure 10, were first proposed for shear wave imaging methods by Sugimoto et al. (Sugimoto et al., 1990) and Sarvazyan et al. (Sarvazyan et al. 1998), and this concept was developed in the context of diagnostic ultrasonic imaging concurrently by several groups in the early 2000s (K. R. Nightingale, McAleavey, & Trahey, 2003; J. J. Bercoff, Tanter, & Fink, 2004; Chen, Fatemi, & Greenleaf, 2004). The propagation speed of shear waves in soft tissue is several orders of magnitude slower than the speed of sound in soft tissue (1-10 m/s compared to 1540 m/s), so ultrasonic correlation and Doppler-based method can be used to monitor their propagation. Equations modeling shear wave propagation can be derived from the constitutive properties reflected in (1) and Newton's 2nd law (conservation of momentum) as shown below:

Table A2. Speckle tracking vs. Doppler method

Method Feature	Spatial correlation method (Speckle tracking method)	Phase difference detection method (Doppler method)
Displacement vector	2D measurement possible	1D displacement (Doppler angular dependency)
Displacement amount	Displacement exceeding wavelength applicable	Up to about half of wavelength (because of aliasing)
Real-time capability	Computational complexity	High-speed operation easy
Noise tolerance	Low	High

$$G\nabla^2 u - \rho \frac{\partial^2 u}{\partial t^2} = 0, \tag{A12}$$

where ρ is the material density (typically assumed to be 1 g/cm³ for soft tissue), u is the tissue displacement, ∇^2 is the Laplacian operator determining the spatial gradients of displacement, G is the shear modulus, and t is time. The shear wave propagation speed that is associated with solving the above wave equation is related to the underlying tissue shear modulus (G), through Eq. (A9) (elastic material assumption, $G = \rho c_s^2$) or Eq. (A10) (which can be derived using viscoelastic material assumptions).

Ideally, shear wave speeds can be reconstructed from 3D displacement data, as is commonly used in magnetic resonance elastography (MRE) (Oliphant, Manduca, Ehman, & Greenleaf, 2001; Sinkus *et al.*, 2000b). Ultrasonic elasticity imaging, however, is generally restricted to a single tomographic imaging plane that does not allow for full 3D displacement monitoring. Additionally,

the presence of jitters in the ultrasonic displacement estimates can yield data with 10-20 dB SNR that is not amenable to second-order differentiation in space and time without excessive amplification of the jitters, leading to exceedingly noisy shear wave speed estimates when employing inversion of Eq. (A12) to determine shear wave speed, as was initially pursued with transient radiation force excitation methods (J. J. Bercoff *et al.*, 2004; K. R. Nightingale *et al.*, 2003). For these reasons, time-of-flight (TOF) methods that perform a linear regression of the wave arrival time versus position data are now typically used.

TOF-based methods employ *a priori* assumptions, including local homogeneity, and a known direction of propagation, such that the arrival time of the wave at adjacent positions can be used to determine the shear wave speed. All of the commercially available methods make assumptions about tissue behavior to generate a shear wave speed estimate, and the accuracy of those assumptions ultimately impacts the accuracy of the resulting estimate.

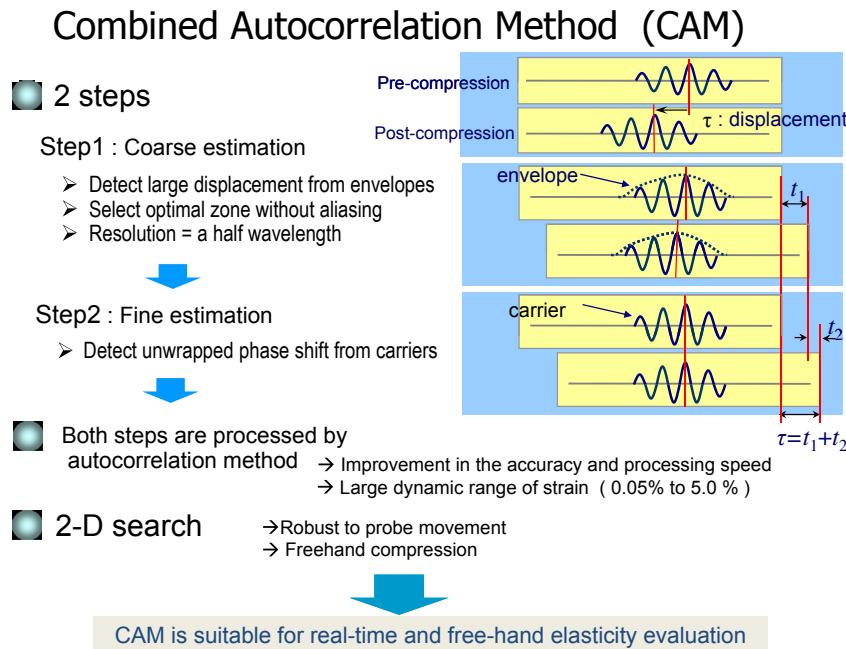


Figure A5. Principle of the combined autocorrelation method. The rough displacement is first calculated from the envelope using the resolution of half a wavelength, and then the displacement is calculated in high resolution using the phase difference after correcting the rough displacement. Because both processes use the autocorrelation method used in color Doppler, it achieves high speed. As a result, it has a wide dynamic range and provides high accuracy, being able to accommodate strain ranging from approximately 0.05% to 5% without causing aliasing errors. Therefore, the method is suitable for manual compression methods. It was installed in the first equipment that was put to practical use, and it is currently being used in a 3D elastography system.